

Superprism phenomena in waveguide-coupled woodpile structures fabricated by two-photon polymerization

Jesper Serbin and Min Gu

CUDOS and Centre for Micro-Photonics, Faculty of Engineering and Industrial Sciences, Swinburne University of Technology, Hawthorn, Victoria 3122, Australia
mgu@swin.edu.au

<http://www.swin.edu.au/optics/cmp>

Abstract: Here we give theoretical as well as experimental evidence for wavelength dependent super-refraction phenomena in waveguide coupled superprisms based on polymer woodpile structures. The photonic crystals were fabricated by means of the two-photon polymerization technique and have a partial band gap at near infrared wavelengths. To visualize the superprism effect the light propagating inside the woodpile structure was imaged using a CCD for a continuous range of wavelengths slightly above the band gap frequency. We were able to demonstrate a change of propagation direction from $+50^\circ$ (positive refraction) to -10° (negative refraction) with respect to the crystal surface normal for a wavelength range between 860 nm and 960 nm. Our results show the great potential of these low refractive index three-dimensional crystals, fabricated in a very fast and single-step process, to serve directly as functional micro-optical devices in the near infrared wavelength regime.

©2006 Optical Society of America

OCIS codes: (230.3990) Microstructure devices; (230.3120) Integrated optics devices.

References and links

1. E. Yablonovitch, "Inhibited spontaneous emission in solid state-physics and electronics," *Phys. Rev. Lett.* **58**, 2059–2062 (1987).
2. S. John, "Strong localization of photons in certain disordered dielectric superlattices," *Phys. Rev. Lett.* **58**, 2486–2489 (1987).
3. S. Fan, P.R. Villeneuve, R.D. Meade, and J.D. Joannopoulos, "Design of three-dimensional photonic crystals at submicron lengthscales," *Appl. Phys. Lett.* **65**, 1466–1468 (1994).
4. E. Yablonovitch, T.J. Gmitter, and K.M. Leung, "Photonic band structure: the face-centered-cubic case employing nonspherical atoms," *Phys. Rev. Lett.* **67**, 2295–2298 (1991).
5. T. Prasad, V. Colvin, and D. Mittleman, "Superprism phenomenon in three-dimensional macroporous polymer photonic crystals," *Phys. Rev. B* **67**, 1651031–1651037 (2003).
6. J. Serbin, and M. Gu, "Experimental evidence for superprism effects in three-dimensional polymer photonic crystals," *Adv. Mater.* **18**, 221–224 (2006).
7. J. Shin, S. Fan, "Conditions for self-collimation in three-dimensional photonic crystals," *Opt. Lett.* **30**, 2397–2399 (2005).
8. Z. Lu, J.A. Murakowski, C.A. Schuetz, S. Shi, G.J. Schneider, D.W. Prather, "Three-dimensional subwavelength imaging by a photonic-crystal flat lens using negative refraction at microwave frequencies," *Phys. Rev. Lett.* **95**, 1–4 (2005).
9. S. G. Johnson, J. D. Joannopoulos, MIT Photonic Bands software, <http://ab-initio.mit.edu/mpb>, 1999.
10. M. Straub, and M. Gu, "Near-infrared photonic crystals with higher-order bandgaps generated by two-photon photopolymerization," *Opt. Lett.* **27**, 1824–1826 (2002).
11. J. Serbin, A. Egbert, A. Ostendorf, and B. N. Chichkov, R. Houbertz, G. Domann, J. Schulz, C. Cronauer, L. Fröhlich, and M. Popall, "Femtosecond laser-induced two-photon polymerization of inorganic-organic hybrid materials for applications in photonics," *Opt. Lett.* **28**, 301–303 (2003).
12. J. Serbin, A. Ovsianikov, and B. Chichkov, "Fabrication of woodpile structures by two-photon polymerization and investigation of their optical properties," *Opt. Express* **12**, 5221–5228 (2004).

13. S. Y. Lin, J. G. Fleming, D. L. Hetherington, B. K. Smith, R. Biswas, K. M. Ho, M. M. Sigalas, W. Zubrzycki, S. R. Kurtz, and J. Bur, "A three-dimensional photonic crystal operating at infrared wavelengths," *Nature* **394**, 251 (1998).
 14. U. Streppel, P. Dannberg, C. Waechter, A. Braeuer, and R. Kowarschik, "Formation of micro-optical structures by self-writing processes in photosensitive polymers," *Appl. Opt.* **42**, 3570-3579 (2003)
 15. J. J. Baumberg, N. M. B. Perney, M. C. Netti, M. D. C. Charlton, M. Zoorob, and G. J. Parker, "Visible-wavelength super-refraction in photonic crystal superprisms," *Appl. Phys. Lett.* **85**, 354-356 (2004).
-

1. Introduction

The concept of photonic crystals (PC's) offers a variety of opportunities for the miniaturization of micro-optical devices and the realization of highly integrated optical circuits, in analogy to microchips in semiconductor electronics. Since the introduction of these concepts [1, 2], researchers have put an enormous effort into the design and realization of PC devices that operate in the near infrared wavelength regime [3, 4]. Until now, investigations on photonic crystal structures mainly aimed the realization of complete photonic band gap (PBG) structures. However, recent publications have shown that even in the absence of a complete PBG, photonic crystals can have unique dispersive properties which are a result of their highly anisotropic and wavelength dependent dispersion surface. This effect leads to a variety of possible applications for low refractive index photonic crystals that do not necessarily have a complete PBG such as superprism devices [5, 6], self-collimation devices [7] or super-lenses [8] based on negative refraction. In our work we investigated the superprism effect in waveguide-coupled polymer woodpile structures theoretically as well as experimentally. For the fabrication of the photonic crystals structures we applied the two-photon polymerization technique which is a method that allows for the rapid fabrication of arbitrary three-dimensional (3D) polymer structures with a resolution of approximately 150 nm. To visualize the directions of propagation of light inside the photonic crystal, we used a CCD to image light that is scattered by imperfections of the crystal lattice and shows the path of the propagating light. The theoretical modelling of the dispersion properties were performed by means of the plane-wave expansion method by using the freely available software package MPB [9].

2. Fabrication of the photonic crystal structures

The two-photon polymerization (2PP) technique is a direct laser writing method that can be used to fabricate 3D structures of arbitrary shape [10-12]. Since the 2PP process has a sharp threshold regarding laser intensity and exposure time, the size of the polymerized structures can be controlled by means of laser power and scanning speed and can be far below the diffraction limit [11]. In 2PP, a photosensitive resin is irradiated by tightly focused, ultrashort laser pulses ($\tau_{\text{pulse}} \sim 100$ fs) at a wavelength that is above the single-photon absorption wavelength, allowing to focus the laser beam into the volume of the resin without having any single-photon induced polymerization reactions. If the light intensity within the focal volume is sufficiently high, the polymerization process can be initialized by two-photon absorption. When moving the laser focus three-dimensionally through the resin, the polymerization will occur along the trace of the laser focus allowing for 3D micro-structuring of arbitrary shapes. The 3D photonic crystal lattice that we chose to demonstrate the superprism effect is the so called woodpile structure (or layer-by-layer structure). The woodpile structure consists of layers of one-dimensional rods with a stacking sequence that repeats itself every four layers. The distance between four adjacent layers is denominated by b . Within each layer, the axes of the rods are parallel to each other with a distance d between them. The adjacent layers are rotated by 90° . Between every other layer, the rods are shifted relative to each other by $d/2$. Generally, the resulting structure has face-centred-tetragonal lattice symmetry. For the special case of $(b/d)^2=2$, the lattice can be derived from a face-centred-cubic (f.c.c.) unit cell with the basis of two rods [13]. Using optically high quality organic-inorganic hybrid polymers

(ORMOCER[®]s) for 2PP we were able to achieve a resolution of ~ 150 nm allowing for the fabrication of woodpile structures with an in-layer rod distance as small as 700 nm.

Figure 1 shows scanning electron microscope (SEM) images of a crystal that was fabricated by means of the 2PP technique. A massive frame was built around the photonic crystal to prevent the structure from collapsing during the development process [10]. The PC was fabricated together with a tapered waveguide structure that allows for coupling light into the photonic crystal at a well defined angle, see Fig. 1(a) and 1(b). Here we chose an angle of 35° with respect to the surface normal. The two facets for coupling the light into the waveguide and into the photonic crystal have a square shape were $13\ \mu\text{m}$ and $4\ \mu\text{m}$ wide, respectively, and the length of the taper was $140\ \mu\text{m}$. As it can be seen Fig. 2(c) and 2(d) the rods of the woodpile structure have an angle of 45° with respect to the crystal surface. Fabricating the waveguide at a distance of less than $5\ \mu\text{m}$ to the edge of the substrate enabled us to couple light into the waveguide with relatively small coupling losses.

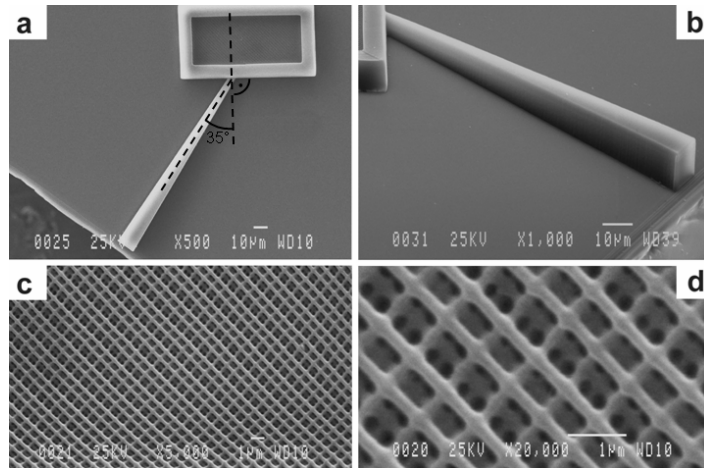


Fig. 1. SEM images of a waveguide-coupled woodpile structure fabricated by means of two-photon polymerization. (a) Overview of the photonic crystal with a massive frame to support the fragile structure and the tapered waveguide used to couple light into the photonic crystal. (b) Detailed view of the waveguide structure. (c) and (d) Details of the woodpile structure.

3. Characterisation of the photonic crystals

By applying the 2PP technique we fabricated woodpile structures having in-layer rod distances between 700 nm and $1.3\ \mu\text{m}$. Their transmission spectra were measured by means of Fourier-transform infrared (FTIR) spectroscopy [6]. The fundamental stop bands were found as transmission dips at wavelengths between $1.21\ \mu\text{m}$ and $1.81\ \mu\text{m}$, respectively. The positions of the band gaps were in good agreement with the calculated band structures, where the fundamental stop band in the (Γ -X)-direction could be found at normalized frequencies d/λ between 0.57 and 0.59.

To visualize the pathways of the light propagating inside the crystal, the top surface of the crystal, which is parallel to the plane to which the propagating light is confined, was imaged onto a CCD camera. A fraction of the propagating light, which is scattered by imperfections in the lattice, is imaged onto the CCD chip, too. This allows to record images of the crystal and the propagating laser light simultaneously. The photographs in Fig. 2 show linearly polarized light of different wavelengths coupled into the woodpile structure via the tapered waveguide (see movie in supplementary information). As the wavelength is tuned from 860 nm to 960 nm, the light inside the crystal changes its direction of propagation by approximately 60° .

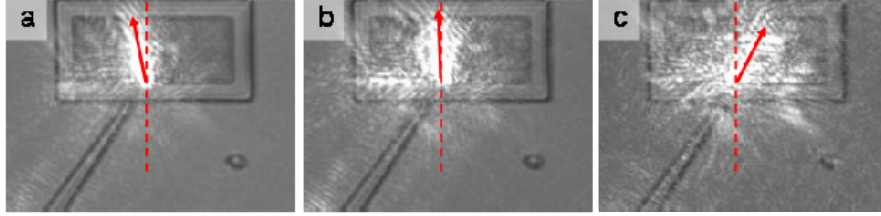


Fig. 2. Microscope images of the waveguide coupled woodpile structure (size: $85 \mu\text{m} \times 45 \mu\text{m}$) and the light propagating inside the photonic crystal. The red dotted line indicates the surface normal and the red arrows show the direction of propagation. (a) $\lambda=960 \text{ nm}$, (b) $\lambda=930 \text{ nm}$, (c) $\lambda=880 \text{ nm}$. The full tuning range (860 nm to 960 nm) can be seen in the movie *sp.mov* (file size: 0.96 MB).

At long wavelengths ($\lambda > 930 \text{ nm}$) the structure shows negative refraction; i.e. light is refracted to the opposite direction compared to the direction of incidence (see Fig. 2(a)). When tuning the laser light to shorter wavelengths, the effective refractive index of the woodpile structures changes to a positive value (Fig. 2(b) and 2(c)).

4. Theoretical modelling of the dispersive properties

To calculate the dispersion properties of the woodpile structure we computed the iso-energy surface (IES) based on the complete three-dimensional band-structure (i.e. the Bloch modes for all k-vectors directing from the Γ -point to any point within the first Brillouin zone) and derived the direction of the group velocity from the gradient of the IES. The calculation of the complete photonic band-structure was performed by applying the freely available software package MPB [9]. The derived function $\omega(|k|, \phi, \theta)$ was then numerically solved for $|k| = |k|(\omega, \phi, \theta)$, where $\omega = d/\lambda$ is the normalized frequency, $|k|$ the magnitude of the k-vector and ϕ and θ are the azimuth angle and elevation, respectively. For a constant frequency ω the function $|k|(\phi, \theta)$ is called iso-energy surface or dispersion surface and is the optical equivalent to the Fermi-surface in crystals [5]. For all of the shown calculations we assumed an infinitely large photonic crystal structure. Effects of the finite size and the refractive index of the substrate material (which was a standard microscope cover glass) were not taken into account.

Since the group velocity of light is equal to $\partial\omega/\partial k$, the direction of propagation inside the PC is normal to the IES and can be derived under the assumption that the parallel component of the k-vector is conserved as the light from one medium into another. The green line in Fig. 3(a) indicates the plane $k_z=0$. When the incident light is parallel to the x-y plane, the light inside the crystal is confined to that plane due to symmetry reasons. The contour in Fig. 3(b) shows the intersection of the IES with the plane $k_z=0$. Since the light is coupled into the woodpile structure by means of a waveguide, we have to consider two interfaces, one between air and the waveguide and one between the waveguide and the photonic crystal. The k-vector for light propagating in each of the domains can be found by taking into account that k_{\parallel} is conserved at each interface and the magnitude of the k-vector is defined by the iso-energy contour of the respective material.

Following this construction scheme, we calculated the angles of light propagating inside the woodpile structure for a range of normalized frequencies.

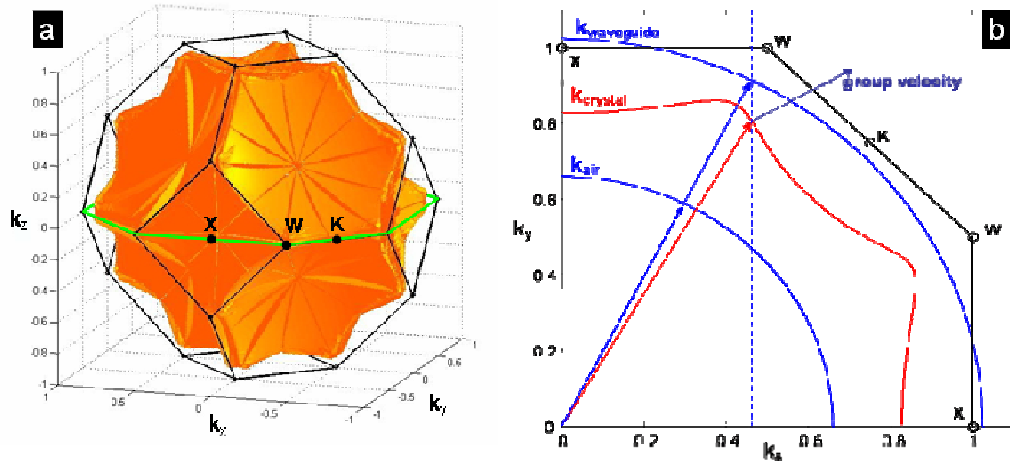


Fig. 3. (a) Calculated iso-energy surface (IES) at a normalized frequency of 0.655 (4th band) for a woodpile structure having a contrast in refractive indices of $n=1.552$ [14]. (b) Iso-energy contour showing an intersection of the IES from (a) with the plane $k_z=0$. The blue contours indicate the dispersion curve for air and the polymer waveguide, the red contour shows the dispersion curve for the photonic crystal structure.

For the given in-layer rod distance of 700 nm, we converted the normalized frequencies into wavelengths and plotted the data together with the experimentally derived angles of propagation (see Fig. 4).

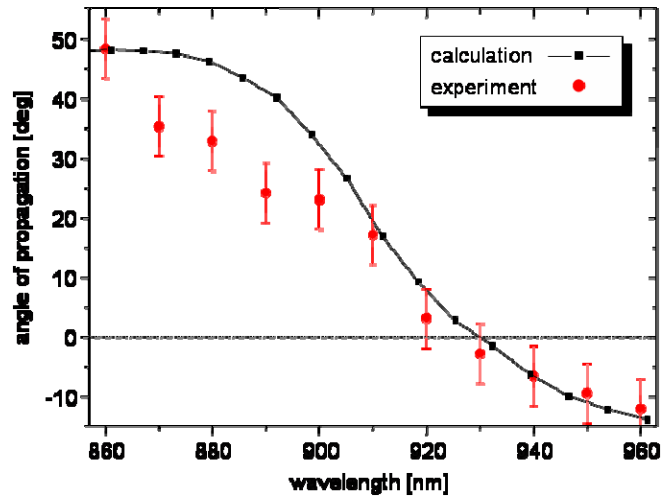


Fig. 4. Measured angles of propagation for light at different wavelengths (red circles) together with the calculated data (black line and squares).

The experimental data are in good agreement with the numerical model and show a change in propagating angle of 60° for a 100 nm change in wavelength. Such a change is approximately two orders of magnitude higher than in conventional prisms [15]. The error bars in Fig. 4 are mainly determined by uncertainties related to the measurement of angles of propagation from the CCD images.

5. Conclusion

We have fabricated waveguide-coupled 3D photonic crystals based on the woodpile structure by means of the two-photon polymerization technique. The crystals have a photonic bandgap at a wavelength of 1.21 μm and show superprism effects at wavelengths slightly below their PBG. We have demonstrated these wavelength dependent dispersion properties experimentally and they are in good agreement with our theoretical calculations. We were able to observe a change in the propagating angle of approximately 60° for a wavelength tuning range of 100 nm. This effect is two orders of magnitude larger than in conventional prisms. Furthermore we could demonstrate wavelength regions of negative as well as positive refraction. The low refractive index 3D PC's, fabricated in a very fast and single-step process, provides potential functional micro-optical devices in the near infrared wavelength regime.

Acknowledgments

This work was produced with the assistance of the Australian Research Council under the ARC Centres of Excellence program. CUDOS (the Centre for Ultrahigh-bandwidth Devices for Optical Systems) is an ARC Centre of Excellence.